Thermal and Thermomechanical Study of Micro-refrigerators on a Chip based on Semiconductor Heterostructures

S. Dilhaire, Y. Ezzahri, S. Grauby, and W. Claeys
CPMOH – University of Bordeaux, 351 cours de la Libération, F-33405 TALENCE
J. Christofferson, Y. Zhang and A. Shakouri
Baskin School of Engineering, University of California, 1156 High St, Santa Cruz, CA 95064

Abstract

We present results from optical characterization of active solid-state SiGe/Si thermionic micro coolers with sizes ranging from 40x40 up to 100x100 micron square. These devices have achieved 7K cooling at 100°C ambient temperature. These micro refrigerators can be used to remove hot spots in IC chips and achieve localized temperature control. Transient thermoreflectance measurements have shown that the cooling speed of these thin film coolers is on the order of 20-30 microseconds, 10^4 times faster than the commercial Bi_2Te_3 thermoelectric coolers.

We characterized several micro-refrigerators devices by various optical non-contact methods such as interferometry or thermoreflectance. Maximum surface temperature and displacement was measured for a variety of devices sizes. The contribution of Peltier/thermoionic effect at interfaces and Joule heating inside the structure were separated by studying their different current dependence. Cooling is proportional to the current while Joule heating is proportional to the square of the current. We found that these two terms have different device size area dependence. This was explained by the fact that cooling occurs on top of the device and thus the cooling temperature is proportional to the sum of the device and substrate thermal resistances while the temperature rise due to Joule heating is only proportional to the substrate thermal resistance. This shows that the dominant source of heat is in the buffer layer below the device or in the substrate itself.

Introduction

With the rapid development of VLSI technology, heat generation and thermal management are becoming one of the barriers to further increase clock speeds and decrease feature sizes. There has been an increasing demand for localized cooling and temperature stabilization of microelectronic and optoelectronic devices. Recently p-type BiTe/SbTe electron transmitting, phonon blocking thin film coolers have been demonstrated with high thermoelectric figure-of-merit and cooling power density [1]. Low dimensional structures have also been extensively studied for their improved performance [2,3]. Si-based microcoolers are attractive for their potential monolithic integration with Si microelectronics. SiGe is a good thermoelectric material especially for high temperature applications [4], and superlattice structures can further enhance the cooler performance by reducing the thermal conductivity between the hot and the cold junctions, and by selective emission of hot carriers above the barrier layers in the thermionic emission process [5,6,7,8]. In this article we present detailed characterization of solid-state thermionic micro coolers using reflectometric and interferometric measurements. These results are compared with ones obtained with micro thermocouples and the contribution of interface Peltier/thermionic cooling is separated from the Joule heating in the device.

1. Sample description

Microcooler samples consisted of a 1μm thick superlattice layer with doping concentration of $5e19cm^{-3}$, a 1μm $Si_{0.8}Ge_{0.2}$ buffer layer with the same doping concentration as the superlattice and a 0.25μm $Si_{0.8}Ge_{0.2}$ cap layer with doping concentration of $5e19$ cm^{-3} [9]. A second cap layer with higher doping concentration ($2e20cm^{-3}$) was included in order to improve the ohmic contact between the metal and semiconductor. The most important part of the device is the superlattice layer. In addition to thermionic emission, it can also reduce the thermal conductivity to prevent the backflow of heat from substrate to cold junction. The buffer layer on top of the Si substrate was included in order to reduce strain due to lattice mismatch between the substrate and the superlattice. The samples were grown in a molecular beam epitaxy (MBE) machine on five inch diameter (001)-oriented Si substrates, p-type doped to 0.003~0.007 Ω-cm with Boron. A Ti/Al/Ti/Au layer was evaporated on top of the samples for electrical contact. Figure1 shows a schematic of cross-section view of the Si/SiGe superlattice micro-cooler. Figure 2 shows an image under Scanning Electron Microscope (SEM).
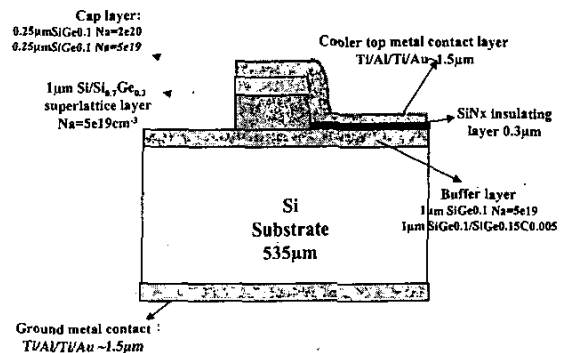

Figure 1: Illustrative cross-section view of Si/SiGe superlattice micro-cooler (Drawing not to scale)

2. Characterization technique

2.1 Micro-thermocouple

The cooling of the devices versus supplied current was measured by standard E-type micro-thermocouple with the tip size of 50μm [9,10]. The ILX Lightwave LDX3220 current source was used to supply the stable current to the cooler

Figure 2: Scanning Electron Microscope (SEM) picture of Heterostructure Integrated Thermoionic (HIT) Micro-coolers

through probes. The thermocouple tips were placed on top of the sample and the substrate. HP 34420A Nanovoltage/microohm-meter was used to measure the voltage difference between the two-thermocouple tips. A LabView™ program was developed to automatically control measurements and convert the voltage difference to temperature by using temperature calibration table offered by the manufacture. A schematic drawing of experimental step-up was illustrated in Figure 3.
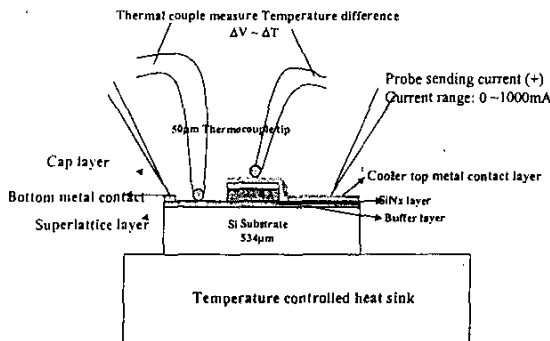

Figure 3: Thermocouple measurements Set-up

2.2 Optical techniques

We have developed two very high resolution laser probes [11,12,13,14] in order to measure the surface temperature variation and the dilation upon running components.

Interferometer

This laser probe is a homodyne stabilized Michelson interferometer shown in figure 4. The laser is a stabilized polarized HeNe laser ($\lambda=632.8$ nm). The beam splitting element of the interferometer is a polarizing prism. By rotating a half wave plate ($\lambda/2$) it is possible to partition the intensity of the reference arm to that of the probe arm so as to equalize the reflected intensities and to obtain high contrast interference fringes. In the reference and probe arm a quarter wave plate ($\lambda/4$) is inserted. The linear polarization of the incoming light is rotated by 90° when coming out as it has passed twice the plate. This allows to reflect all the intensity of the returning beams to the photodetector and the polarizing prism acts as an optical insulator. The two beams have orthogonal linear polarizations. To obtain interferences, both polarizations are projected at 45° upon a same axis by passing through a polarizing beam splitter (prism) before the photodetector.

A microscope objective focuses the probe beam upon the surface of the component under test. The phase of the reflected beam is modulated by the surface normal displacements. The sample is mounted on a 3-D micrometric translation stage. The laser impact upon the sample can be viewed on a CCD camera by moving the mirror in front of the reflected probe beam and by reducing the laser beam intensity with the attenuation placed in the laser beam. The lateral resolution is 1 µm. The interferometer is actively stabilized at the point of highest sensitivity (mid-fringe).
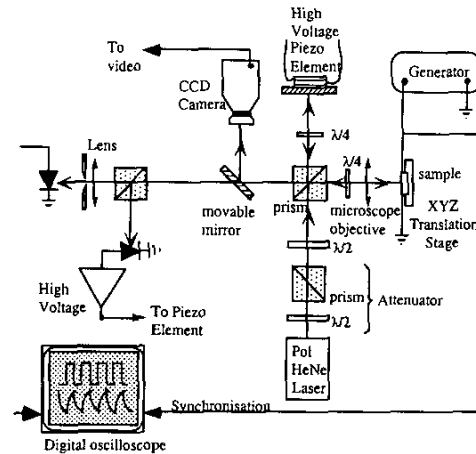

Figure 4: Schematic view of laser probe

The detected signal is averaged in synchronism with the excitation signal and recorded by a digital oscilloscope or by a lock-in amplifier for sinusoidal excitation. Absolute values of the surface displacement are obtained from comparison of the photodetected signal amplitude with the fringe signal amplitude from large displacements produced by moving the piezomirror in the reference arm. It is very important to notice that the measurements of surface displacement obtained this way are absolute and perfectly reproducible within a few percents.

Reflectometer

Changes in the temperature of semiconductors or metals, lead to changes in their reflectivity, this is thermoreflectance. We exploit this phenomenon in a laser probe to measure the thermal changes of normally working integrated circuits.

When a material (semiconductor or metal) undergoes a temperature change T, its reflection coefficient (for normal incidence and fixed wavelength) undergoes a corresponding change R. We develop R in powers of T:

$$\Delta R = a\Delta T + b(\Delta T)^2 + ... \qquad (1)$$

For small temperature changes we limit the development to:

$$\Delta R = a\Delta T = \frac{\partial R}{\partial T}\Delta T \qquad (2)$$

If we focus a laser beam of intensity Φ_0 onto the material and detect with a photodiode the reflected light intensity $R\Phi_0$, the measured current is proportional to $R\Phi_0$ and can be written: $I = SR\Phi_0$ $\qquad (3)$

If we measure the current change I associated to the temperature change T, as shown in figure 5, then:

$$\frac{\Delta I}{I} = \frac{\Delta R}{R} = \frac{1}{R}\frac{\partial R}{\partial T}\Delta T \qquad (4)$$

So that:

$$\Delta T = \left(\frac{1}{R}\frac{\partial R}{\partial T}\right)^{-1}\frac{\Delta I}{I} = \kappa\,\frac{\Delta I}{I} \qquad (5)$$
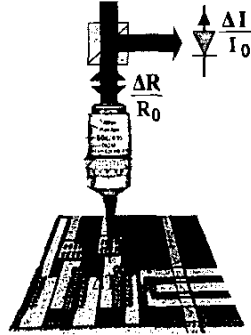
Figure 5: Thermoreflectance principle

We see that with a simple optical probe it is possible to measure dynamic temperature changes. Absolute values are readily obtained if $\kappa = \dfrac{1}{R}\dfrac{\partial R}{\partial T}$, the relative reflectance temperature coefficient, is known. The experimental set-up is the same as the one described in figure 4 with the difference that no light is send in the reference arm. No interferences occur and the detector measures amplitude changes of the reflected laser beam. Experimentation shows the device to be a simple and excellent tool for integrated circuit surface temperature variation measurements. The optical probe is capable to measure surface temperature changes in the range 10^{-3}- 10^{2} K at micrometric scale upon integrated circuits. High resolution temperature mapping can be realized and dynamic responses can be studied in the DC - 150 MHz range with our detection system.

3. Experimental results

3.1 Cooling versus current for different device sizes

Our thermocouple has a resolution of 0.05^{0}C temperature measurement. It is a convenient and quick method to evaluate our micro-cooler device. However, one minor drawback for this method is for smaller device less than $50\times50\mu m^{2}$, the heat load from the thermocouple will have a significant influence on measurements. The measured results for smaller devices less than $50\times50\mu m^{2}$ will be about 10% lower than the actual device cooling. However, for devices larger than $50\times50\mu m^{2}$, the measured cooling will be exact the actual device cooling. This similar trend is confirmed with our observation when comparing 1D simulation and thermo-reflectance results with thermo-couple measurements for other sample. Figures 6 and 7 show respectively thermocouple and thermoreflectance measurements of the cooling of the micro refrigerator versus electrical current for different device sizes. It is clearly shown

that the contact measuring method under estimate the temperature for the smallest device $40\times40\mu m^{2}$.

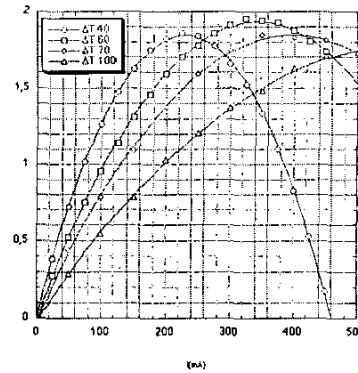Figure 6: Cooling temperature measured by a micro thermocouple upon $40\times40\mu m^{2}$, $60\times60\mu m^{2}$, $70\times70\mu m^{2}$, $100\times100\mu m^{2}$ area micro coolers.
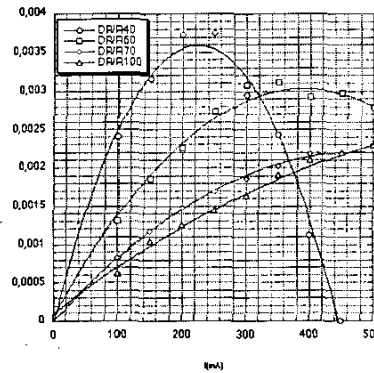
Figure 7: Thermoreflectance signal proportional to the cooling temperature measured upon $40\times40\mu m^{2}$, $60\times60\mu m^{2}$, $70\times70\mu m^{2}$, $100\times100\mu m^{2}$ area micro coolers.

3.2 Peltier/thermionic and Joule contribution versus time

At small current densities, in linear transport regime, one can define an "effective" Peltier coefficient for the superlattice material. In this case interface cooling depends linearly on the current. Joule heating in various layers has a quadratic dependence on current, so the contribution of these two terms can be independently studied by fitting the cooling versus current curve with a quadratic equation. In the case of transient excitation we cam add and subtract the responses obtained from the two current polarities. The Sum gives twice the Joule response, while the difference gives twice the Peltier response. In sine wave excitation, Peltier produces a response at the same frequency as the current, while the Joule response is at twice the frequency. A lock-in amplifier selects the response.

Temperature and dilation have been studied in transient regime. The micro cooler was fed by 2ms current pulses with 100Hz repetition rate. Peltier and Joule responses have been recorded respectively by thermoreflectance and

interferometry. The results are reported in figure 8 and 9. As one can see a quasi steady state is reached by the thermoreflectance response which is related to surface temperature variation. In contrast the dilation does not reach any steady state value. This is due to the fact that the heat flux front propagates towards the substrate and it keeps contributing to the normal surface expansion. The dilation integrates in first approximation the temperature field below the probed point.

From the thermoreflectance response one can easily deduce the time constant of the device, which is about 10μs. This result is in good agreement with the frequency bandwidth presented in the next section.The maximum dilation amplitude reached by the Joule response is about 16nm. This expansion is too much high to be the lonely contribution of the micro cooler. This clearly shows the penetration of the thermal wave into the substrate.
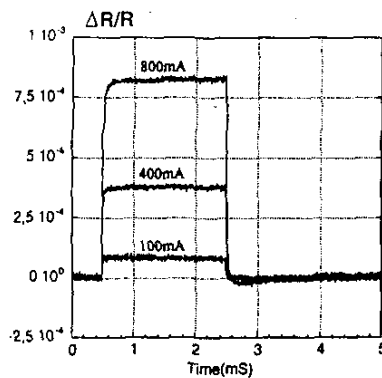

Figure 8: Peltier thermoreflectance response for a 2ms current pulses (100, 400 and 800 mA)
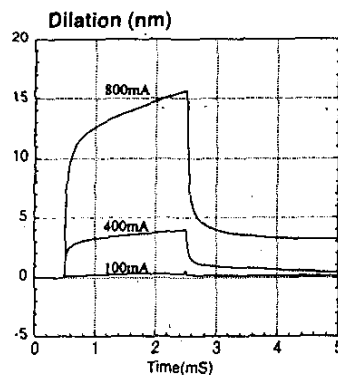

Figure 9: Joule dilation response for a 2ms current pulses (100, 400 and 800 mA)

3.3 Frequency response

The normalized frequency response of the cooling signal for thin film micro coolers of different sizes is presented in figure 8. The thermal transient of 10-20 microseconds is on the order of 10^4 times faster then conventional Bi_2Te_3 coolers. This makes the thin film cooler very attractive for use in a temperature control feedback loop, as the short time scale for

temperature stabilization is critical in sensitive optoelectronic applications.

One can see in figure 10, that the frequency response of Peltier/Thermoionic cooling is on the order of 20kHz. This corresponds to a time response of ~50μs. We can also see that the frequency response is independent of the size device in 40 - 60μm diameter range. This is due to the fact that speed of the device is dominated by the superlattice layer thickness (~3μm) and by the thermal diffusivity of the top metal layer.
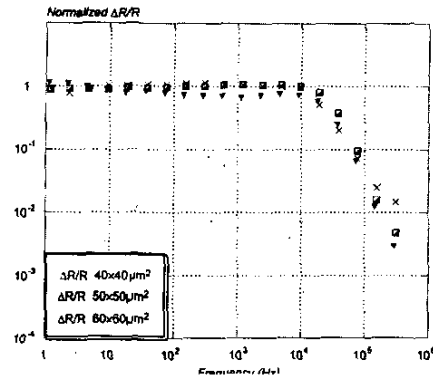

Figure 10: Normalized Peltier efficiency response for $40 \times 40 \mu m^2$, $50 \times 50 \mu m^2$, $60 \times 60 \mu m^2$

4. Discussion

For the cooling efficiency the main limiting factor is the total thermal resistance between the top side of the cooler and the and the heat sink at the back side of the substrate. Detailed simulation have shown that the thermal resistance of the cooler is inversely proportional to its area (A) $R_{cooler} \propto \dfrac{1}{A}$, while the thermal resistance of the substrate is inversely proportional the square root of A: $R_{sub} \propto \dfrac{1}{\sqrt{A}}$

Then the cooling temperature can be expressed as following:

$$\Delta T \cong (R_{cooler} + R_{sub})\left(T_0 SI - \frac{\rho L}{A} I^2 \right) \qquad (6)$$

where T_0 (K) is the room temperature, S the Seebeck coefficient (V/K), ρ the electrical resistivity (Ω.m), L (m) the height of the micro cooler, A its area (m²) and I the electrical current (A).

Thus the dilation (ΔI) and the temperature variation (ΔT) can be fitted with:

$$\Delta I \propto \Delta T \cong \left(\frac{K_1}{\sqrt{A}} + \frac{K_2}{A} \right) + \left(\frac{K_1}{\sqrt{A}} + \frac{K_2}{A} \right)\frac{K_3}{A} I^2 \qquad (7)$$

We present in the following sections the Peltier and Joule area dependence for both thermoreflectance and dilation signals.

4.1 Peltier Area dependence

We have plotted in figure the first term of equation 7 versus the area of the device (A). It represents the contribution

of Peltier cooling. The red curve corresponds to the thermoreflectance signal and the blue one to the dilatation. Each curves match very well with a $\left(\dfrac{K_1}{\sqrt{A}}+\dfrac{K_2}{A}\right)$ fit. It means that both contributions of the substrate and the cooler thermal resistance appears, while the Peltier source is located on top of the cooler.
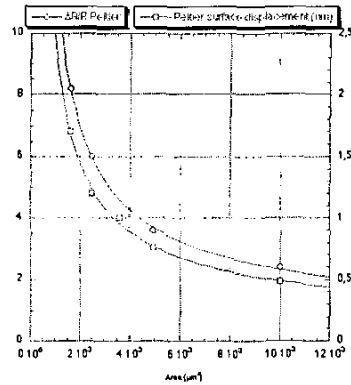

Figure 11: Peltier area dependence. Thermoreflectance signal and dilation well fitted with

$$\frac{\Delta R}{R}=\left(\sqrt{\frac{2.8\,10^4}{A(\mu m^2)}}+\frac{6.4\,10^3}{A(\mu m^2)}\right),\ \Delta l(nm)=\left(\sqrt{\frac{1.3\,10^3}{A(\mu m^2)}}+\frac{1.2\,10^3}{A(\mu m^2)}\right)$$

4.2 Joule Area dependence

The Joule responses have strong different behavior as one can see in figure 10. Data fit very well with $\left(\dfrac{K}{A\sqrt{A}}\right)$. It simply means that the joule heating is only led by the thermal resistance of the substrate (R_{sub}). This allows to locate the Joule source below the microcooler in the buffer layer.
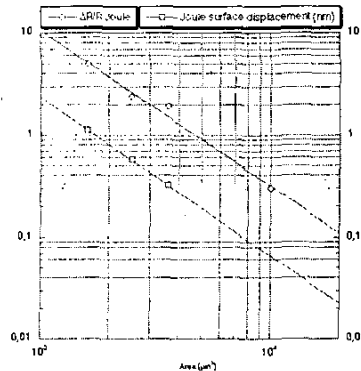

Figure 12: Joule area dependence. Thermoreflectance signal and dilation well fitted with

$$\frac{\Delta R}{R}=\left(\frac{7.2\,10^4}{A^{3/2}(\mu m^2)}\right),\ \Delta l=\left(\frac{3.2\,10^5}{A^{3/2}(\mu m^2)}\right)$$

Conclusion

In this paper we presented detailed characterization of micro-refrigerators using thermocouple, thermoreflectance and interferometric measurements. Maximum surface temperature and displacement was measured for a variety of devices sizes. The contribution of Peltier/thermoionic effect at interfaces and Joule heating inside the structure were separated by studying their different current dependence. Cooling is proportional to the current while Joule heating is proportional the square of the current. We found different device size area dependence for the two terms. This was explained by the fact that cooling occurs at the top of the device and thus the cooling temperature is proportional to the sum of device and substrate thermal resistance while the temperature rise due to Joule heating is only proportional to the substrate thermal resistance. This shows that the dominant source of heat is in the buffer layer below the device or in the substrate itself.

References

1 R. Venkatasubramanian et al, Nature, Vol. 413 (2001), pp. 597-602.

2 L. D. Hicks et al, Phys. Rev. B (Condensed Matter),.Vol. 47 (1993), pp. 12727-31.

3 T. Koga et al, Appl. Phys. Lett., Vol. 77 (2000), pp. 1490-1492.

4 J. B. Vining, J. Appl. Phys, Vol. 69 (1991), pp. 331-341.

5 A. Shakouri et al, Appl. Phys. Lett., Vol. 71(1997), PP. 1234.

6 A. Shakouri et al, Mater. Res. Soc. Symp. Proc. , Vol. 545 (1999), pp. 449.

7 A. Shakouri et al, 16th Int. Conf. on Thermoelectrics, Dresden, Germany, Aug. 1997, pP. 636-640.

8 A. Shakouri et al, Next Generation Materials for Small-Scale Refrigeration and Power Generation Applications Symposium, Boston, MA, USA, Dec. 1998, pP. 449-458.

9 X. Fan et al, Appl. Phys. Lett., Vol. 78(2001), pp. 1580-1582.

10 C. LaBounty et al, J. of Appl. Phys., Vol. 89(2001), pp. 4059-4064.

11 S. Dilhaire et al, "Surface displacement imaging by interferometry with a light emitting diode", Applied Optics, Vol. 41, No.24 (2002), pp. 4996-5001.

12 W. Claeys et al, "Laser Probes for the Thermal and Thermomechanical Characterisation of Microelectronic Devices", Microelectronics Journal, Vol. 32(2001), pp. 891-898.

13 S. Dilhaire et al, "Optical method for the measurement of the thermomechanical behaviour of running electronic devices", Microelectronics reliability, Vol 39(1999), pp. 981-985.

14 J. Christofferson et al, 17th Annual IEEE Semiconductor Thermal Measurement and Management Symposium, San Jose, CA, USA, March 2001, pp. 58-62.